ORIGINAL PAPER

Carl Spandler · Jörg Hermann · Richard Arculus
John Mavrogenes

Redistribution of trace elements during prograde metamorphism from lawsonite blueschist to eclogite facies; implications for deep subduction-zone processes

Abstract The transfer of fluid and elements from sub-ducting crust to the overlying mantle wedge is a fundamental process affecting arc magmatism and the chemical differentiation of the Earth. While the production of fluid by breakdown of hydrous minerals is well understood, the liberation of trace elements remains generally unconstrained. In this paper, we evaluate the behaviour of trace elements during prograde metamorphism and dehydration using samples of high-pressure, low-temperature metamorphic rocks from New Caledonia. Samples examined include mafic and pelitic rock-types that range in grade from lawsonite blueschist to eclogite facies, and represent typical lithologies of subducting crust. Under lawsonite blueschist facies conditions, the low temperatures of metamorphism inhibit equilibrium partitioning between metamorphic minerals and allow for the persistence of igneous and detrital minerals. Despite this, the most important hosts for trace-elements include lawsonite, (REE, Pb, Sr), titanite (REE, Nb, Ta), allanite (LREE, U, Th), phengite (LILE) and zircon (Zr, Hf). At epidote blueschist to eclogite facies conditions, trace-element equilibrium may be attained and epidote (REE, Sr, Th, U, Pb), garnet (HREE), rutile (Nb, Ta), phengite (LILE) and zircon (Zr, Hf) are the major trace-element hosts. Chlorite, albite, amphibole and omphacite contain very low concentrations of the investigated trace elements. The

comparison of mineral trace-element data and bulk-rock data at different metamorphic grades indicates that trace elements are not liberated in significant quantities by prograde metamorphism up to eclogite facies. Combining our mineral trace-element data with established phase equilibria, we show that the trace elements considered are retained by newly-formed major and accessory minerals during mineral breakdown reactions to depths of up to 150 km. In contrast, significant volumes of fluid are released by dehydration reactions. Therefore, there is a decoupling of fluid release and trace element release in subducting slabs. We suggest that the flux of trace elements from the slab is not simply linked to mineral breakdown, but results from complex fluid-rock interactions and fluid-assisted partial melting in the slab.

C. Spandler (✉) · R. Arculus · J. Mavrogenes
Department of Geology,
Australian National University,
0200 Canberra, Australia
E-mail: carl@geology.anu.edu.au

J. Hermann · J. Mavrogenes
Research School of Earth Sciences,
Australian National University,
0200 Canberra, Australia

Introduction

The Earth's convergent plate boundaries not only represent sites where oceanic crust is recycled back into the mantle, but are also responsible for the generation of new crust in associated magmatic arcs (Taylor and McLennan 1985). It is widely accepted that hydrous fluid sourced from dehydrating subducting crust promotes melting in the mantle wedge and the formation of arc magmas. Experimental (Pawley and Holloway 1993; Peacock 1993; Liu et al. 1996; Schmidt and Poli 1998) and geophysical (Lin et al. 1999) studies have confirmed that large volumes of water may be liberated from the downgoing plate as hydrous minerals break down during conversion from blueschist to eclogite-facies mineral assemblages.

Trace element liberation accompanying mineral dehydration is often invoked to explain the distinctive enrichment of large-ion lithophile elements (LILE; Cs, Rb, Ba, Sr, Pb) and light-rare earth elements (LREE) relative to high-field strength elements (HFSE; Ti, Nb, Ta, Zr, Hf) found in arc magmas (Tatsumi et al. 1986; Brenan et al. 1995; Kogiso et al. 1997; Becker et al.
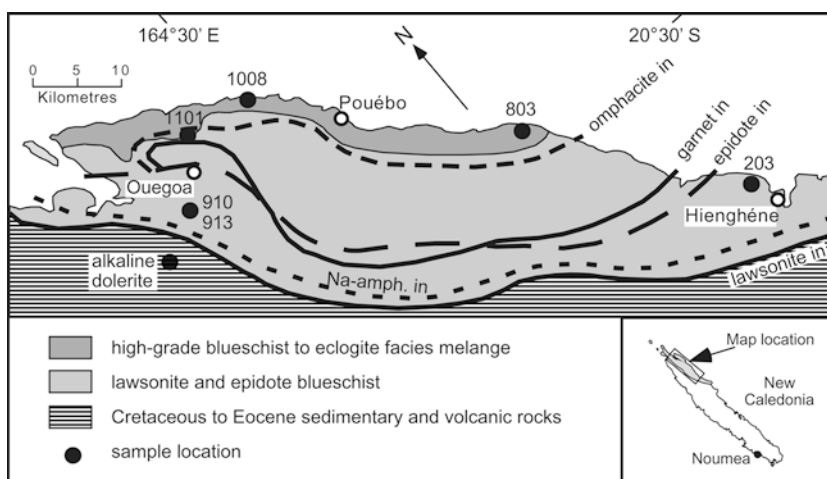
Fig. 1 Simplified geological map of the high-pressure belt of northern New Caledonia. Also shown are the location of samples used in this study and metamorphic isograds. Isograd and geology data from Maurizot et al. (1989), Yokoyama et al. (1986), Black (1977) and Brothers (1985)

2000). There are a range of minerals that may be important for hosting water and trace elements in subducting crust. Of particular interest are calcium aluminosilicate phases such as lawsonite and the epidote-group minerals. These phases may be stable in mafic rocks to pressures in excess of 5 GPa (Ono 1998; Schmidt and Poli 1998; Okamoto and Maruyama 1999; Hermann 2002) and may contain significant amounts of elements such as Sr, Th, U and REE (Domanik et al. 1993; Tribuzio et al. 1996; Ueno 1999; Hermann 2002; Zack et al. 2002). However, in general there is a lack of data concerning the trace element composition of lawsonite, epidote and other high-pressure metamorphic minerals from both mafic and pelitic rock-types (Tribuzio et al. 1996; Arculus et al. 1999). Furthermore, little is known quantitatively of the behaviour and redistribution of trace elements during mineral dehydration.

In north-eastern New Caledonia lies one of the world's largest and most continuous sequences of high-pressure metamorphic rocks. The sequence contains a large variety of lithologies that have recrystallised over a range of metamorphic conditions, and is an excellent analogue of oceanic crust that was subducted to depths of up to 70 km (Aitchison et al. 1995; Clarke et al. 1997). This paper investigates the distribution of trace elements within mineral assemblages from mafic and pelitic rock samples from New Caledonia. These rocks range in grade from lawsonite-blueschist to eclogite-facies and permit identification of the important trace-element-hosting minerals, and evaluation of the fate of trace elements during high-pressure prograde metamorphism. This information is critical for understanding how elements are transported from the slab to the mantle wedge and how arc magmas attain their distinctive trace-element composition.

Geological setting

An extensive (~2,200 km²) belt of high-pressure metamorphic rocks is exposed in north-eastern New Caledonia. The belt is interpreted to have formed during Eocene subduction of an oceanic basin, causing recrystallisation of sedimentary and volcanic protoliths under blueschist- and eclogite-facies conditions (Aitchison et al. 1995; Clarke et al. 1997). A progressive increase in metamorphic grade is observed through the belt and a number of metamorphic isograds have been mapped on the basis of mineral assemblages (Fig. 1; Black 1977; Yokoyama et al. 1986). However, the apparent rapid increase in metamorphic grade is largely due to extensive disruption of the original sequence by exhumation-controlled normal faulting (Rawling and Lister 1999; 2002). Protoliths of the lawsonite and epidote blueschists include a sequence of Cretaceous sandstones, siltstones and cherts with minor basaltic dykes, rhyolite flows and carbonates (Brothers 1985). Stratiform Cu-Pb-Zn (Au, Ag) mineralisation is associated with carbonate schists and some of the rhyolitic flows (Briggs et al. 1977). The highest grade rocks are found in the north-east of the belt and include hornblende-bearing eclogite, garnet-bearing epidote blueschist and quartz-mica schist. Blocks of these rock-types occur within a highly sheared pelite and serpentinite matrix (Maurizot et al. 1989; Rawling and Lister 1999; 2002). Metamorphic conditions range from 0.7–0.9 GPa, 250–400 °C for lawsonite blueschist (Black 1974; Clarke et al. 1997) to 1.6–1.9 GPa, 550–650 °C for eclogite and garnet-bearing epidote blueschist (Carson et al. 1999; Fitzherbert et al. 2001).

Sample description

Six blueschist to eclogite samples were studied to assess the distribution of trace elements within representative rock-types of subducting oceanic crust during prograde metamorphism. Metamorphic facies are defined according to Evans (1990). Properties of these samples are presented in Table 1 and described below. Lawsonite is expected to greatly influence the rheology (Abers 2000; Connolly and Kerrick 2002) and water and trace element budgets (Tribuzio et al. 1996; Schmidt and Poli 1998, Okamoto and Maruyama 1999) of subducting

Table 1 Mineralogical and metamorphic properties of samples examined in this study

Sample	Rock type	Mineral assemblage[a]			Calculated H_2O content[b]	LOI[c]	Pressure (GPa)	Temperature (°C)	Source[d]
		Igneous	Peak metamorphism	Retrograde					
Lawsonite blueschist									
913	Mafic	aug [10]	laws [27], gl [30], qtz [10], alb [4], chl [15], tnt [4], all [t] zrc [t]		5.47	4.95	0.8–1.0	350–400	1
203	Mafic	aug [2], parg [32]	laws [10], gl [12], qtz [6], tnt [4], chl [8], py+cpy [1] zrc [t]	pmp [10], alb [6], hbl [10], apa [0.5], *chl [8]*	3.73	3.66	0.8–1.0	350–400	1
910	Pelite		alb [32], phg [26], qtz [27.5], chl [10.5], laws [1], tnt [1.7], apa [0.5], clc [1], zrc [t]		2.92	2.93	0.8–1.0	350–400	1
Garnet-bearing epidote blueschist									
1101	Alkaline Mafic		phg [22], gl [53] gt [10], ep [5], ap [2], rt [t], zrc [t], qtz [t]	tnt [6]	2.22	2.07	1.6–1.8	550–600	2, 3
Eclogite									
803	Mafic		gl [28], omp [30], gt [20], zoi [11], qtz [6], rt [1.8], py [t], zrc [t]	tnt [t]	0.82	0.51	1.6–1.9	520–580	2, 3
Quartz-phengite schist									
1008	pelite		qtz [46.5], phg [37], hbl [8.5], gt [6], ep [0.5], rt [0.3], apa [0.3], zrc [t]	gl [1]	1.82	2.09	1.6–1.9	550–620	2, 3

[a]Numbers in brackets refers to modal percentage; *t* trace. Mineral abbreviations; *aug* augite, *parg* pargasite, *laws* lawsonite, *gl* glaucophane; *qtz* quartz, *alb* albite, *chl* chlorite, *tnt* titanite, *all* allanite, *zrc* zircon, *py* pyrite, *cpy* chalcopyrite, *pmp* pumpellyite, *hbl* hornblende, *apa* apatite, *phg* phengite, *clc* calcite, *gt* garnet, *ep* epidote, *rt* rutile, *omp* omphacite, *zoi* zoisite
[b]H_2O content calculated from mineral compositions (Table 3) and mineral modes

[c]LOI values from Table 2
[d]Sources of pressure and temperature estimates for peak metamorphism include; *1* Black (1977) and Clarke et al. (1997); *2* Carson et al. (1999) and Fitzherbert et al. (2001); *3* temperatures calculated from garnet-clinopyroxene (Ellis and Green 1979), garnet-amphibole (Graham and Powell 1984) and garnet phengite (Green and Hellman 1984) thermometry

slabs. Therefore, we have chosen to investigate three samples of lawsonite blueschist that are expected to have reached peak metamorphic conditions of 0.7–0.9 GPa, 250–400 °C (Black 1974; Clarke et al. 1997). Sample 913 is a medium-grained, unfoliated mafic rock that consists of prismatic lawsonite grains intergrown with acicular sodic amphibole crystals, chlorite, quartz, albite and fine-grained titanite (Fig. 2A). Although partially replaced, original grains of igneous augite are preserved within the rock. Rare grains of allanite (< 30 μm) also occur in the groundmass (Fig. 2B). Allanite often contains abundant micron-sized inclusions of quartz and has thin zoisite rims. Retrograde metamorphism is restricted to minor replacement of lawsonite by chlorite and actinolite.

Sample 203 is also mafic in composition but is mineralogically and texturally much more complex. Mineral assemblages formed under at least three different metamorphic conditions are preserved in the rock. Coarse-grained igneous pargasite and augite have been altered to hornblende and sodic amphibole, but large zones of fresh pargasite are preserved. The peak blueschist-facies mineral assemblage includes fine-grained titanite, ferro-glaucophane and chlorite and large euhedral porphyroblasts of lawsonite. Greenschist-facies retrogression is manifest as pseudomorphs of lawsonite porphyroblasts by pumpellyite and apatite (Fig. 2C) and replacement of titanite and glaucophane by hornblende and albite. Chlorite appears to have been stable in both metamorphic assemblages. Accessory minerals include subhedral pyrite and chalcopyrite grains and small zircons (< 10 μm) that occur throughout the groundmass.

Lawsonite is usually associated with blueschist-facies mafic to intermediate rocks (Poli and Schmidt 1995; Okamoto and Maruyama 1999) yet it is an important constitute of many pelitic blueschists from New Caledonia (Black 1977). Sample 910 is a pelitic blueschist that contains unaltered porphyroblasts of lawsonite within a fine-grained foliated matrix of quartz, albite, phengite and chlorite. Phases such as calcite, titanite,

**Fig. 2 A** Photomicrograph of mafic sample 913 under transmitted light.
B Backscattered SEM image of an allanite grain in 913.
C Photomicrograph of mafic sample 203 under transmitted light. Light-coloured porphyroblasts are lawsonite partially replaced by pumpellyite and apatite. The groundmass consists of fine-grained chlorite, glaucophane, hornblende, titanite, albite, pargasite, and quartz. The circled opaque grains are pyrite and chalcopyrite.
D Backscattered SEM image of a zoned allanite/zoisite grain from mafic sample 1101.
E, F Backscattered SEM image of zoned allanite/zoisite grains from pelitic sample 1008. Mineral abbreviations as in Table 1
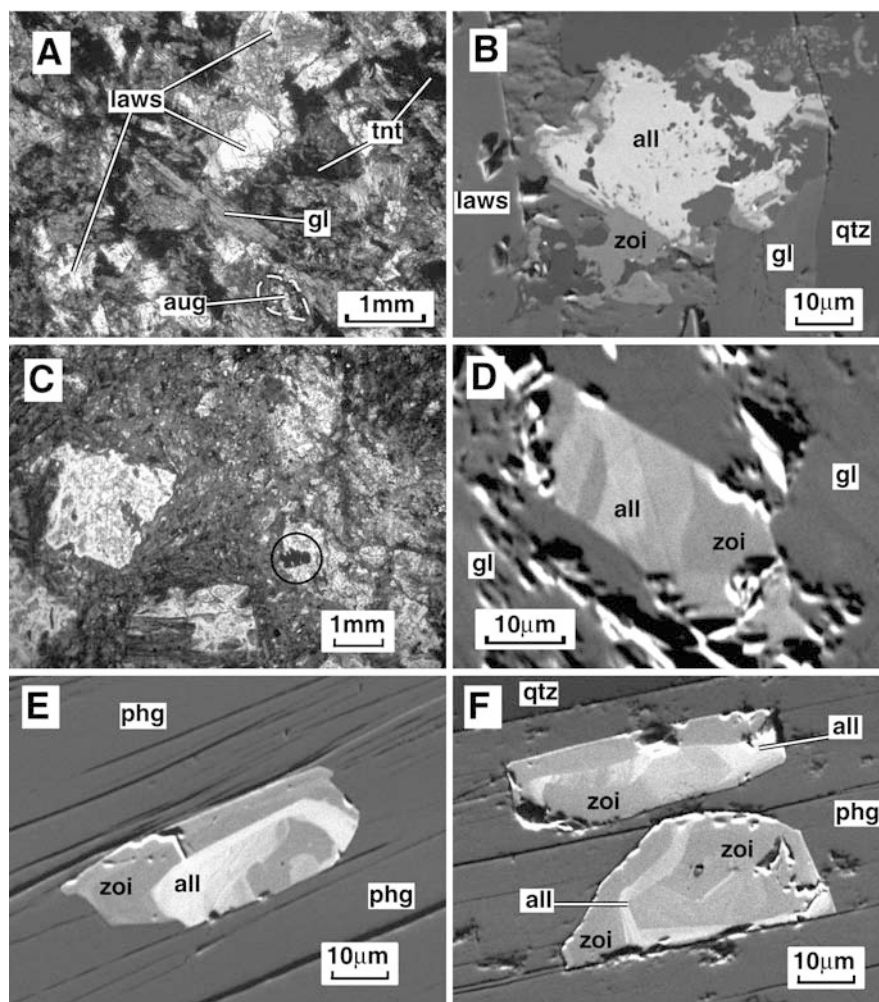
apatite and zircon are a minor component of the rock. The total mineral assemblage has been unaffected by retrogression.

To investigate trace element characteristics at higher metamorphic grades we have selected three samples for detailed study; a garnet-bearing epidote blueschist, an eclogite and a quartz-mica metapelite. The garnet-bearing epidote blueschist sample (1101) is coarse-grained, well foliated and is mineralogically dominated by glaucophane and phengite, reflecting its relatively alkaline composition. Garnet, titanite, epidote and apatite comprise the remainder of the rock. Garnet occurs as coarse idioblastic grains containing inclusions of albite, chlorite, epidote, titanite, rutile and quartz. Rutile also occurs as fine grains mantled by retrograde titanite and as inclusions in phengite. Zircon is present in trace amounts, and is often associated with titanite and rutile. Epidote grains may also be enveloped by retrograde titanite but more commonly form discreet grains with complex zoning between allanite and zoisite (Fig. 2D). Again the allanite/zoisite grains may contain quartz inclusions.

Sample 803 is an unfoliated eclogite consisting of 1–2 mm grains of porphyroblastic garnet, quartz and tabular zoisite set in a fine-grained matrix of glaucophane and omphacite. Paragonite, phengite, pyrite, rutile and zircon are also present in minor or trace amounts. Garnets are zoned and contain an assemblage of mineral inclusions that is the same as the groundmass assemblage. Retrogression is limited to thin titanite overgrowths on rutile.

The sixth sample (1008) examined for this study represents a high-grade equivalent to the pelitic sample 910. Sample 1008 is a coarse-grained, strongly foliated schist dominated by quartz and phengite. Idioblastic garnet and hornblende are the only other major mineral components. Glaucophane occurs as rims on hornblende and is interpreted to be retrogressive. Accessory minerals include apatite, rutile, zircon and epidote. As with samples 1101, the epidote grains are multiply zoned between zoisite and allanite (Fig. 2E, F).

Analytical techniques

Australian National University (ANU). All other trace element concentrations were determined on fused discs by laser ablation, inductively-coupled plasma mass spectrometry (LA ICP-MS) at the Research School of Earth Sciences (RSES), ANU. The LA ICP-MS employs an ArF (193 nm) EXCIMER laser and a Fisons PQ2 STE ICP-MS. A spot size of 100 μm was used and the counting time was 40 s for the background and between 80–120 s for sample analysis. Instrument calibration was against NIST 612 glass using the reference values presented in Table 2. ^{43}Ca was employed as the internal standard isotope, based on CaO concentrations previously measured by XRF. Loss-on-ignition (LOI) values were calculated from the mass difference to 2 g of powdered sample after heating to 1010 °C for one hour.

Major-element mineral compositions were determined from rock thin sections using an energy-dispersive spectrometer (EDS) equipped, JEOL 6400 scanning electron microscope (SEM), housed

at the Research School of Biological Sciences, ANU. Accelerating voltage, beam current and counting time were set at 15 kV, 1 nA and 100 s respectively. Allanite grains in samples 913 and 1008 were analysed at the RSES by wavelength dispersive spectrometry using a Cameca SX 100 electron microprobe. Acceleration voltage was again set to 15 kV, beam current was 20 nA and the total counting time was 307 s. Rare earth elements and Y were standardised using a set of pure REE and Y phosphates synthesised by the Chinese Ceramic Society. Synthetic ThO_2 and $(Sr,Ba)Nb_2O_6$ were used as standard for Th and Sr respectively.

Mineral trace elements were acquired in-situ by LA ICP-MS under similar running conditions to those described above, although spot sizes varied from 65 to 23 μm. All minerals were quantified using either ^{43}Ca or ^{27}Al as the internal standard isotope, except rutile for which ^{49}Ti was employed. Mineral grains were chosen to avoid mineral inclusions during analysis. However,

Table 2 Whole-rock geochemistry of the examined samples. Also shown are the NIST 612 values used for LA-ICP MS data reduction. Major elements expressed as weight percent oxides, trace elements in ppm

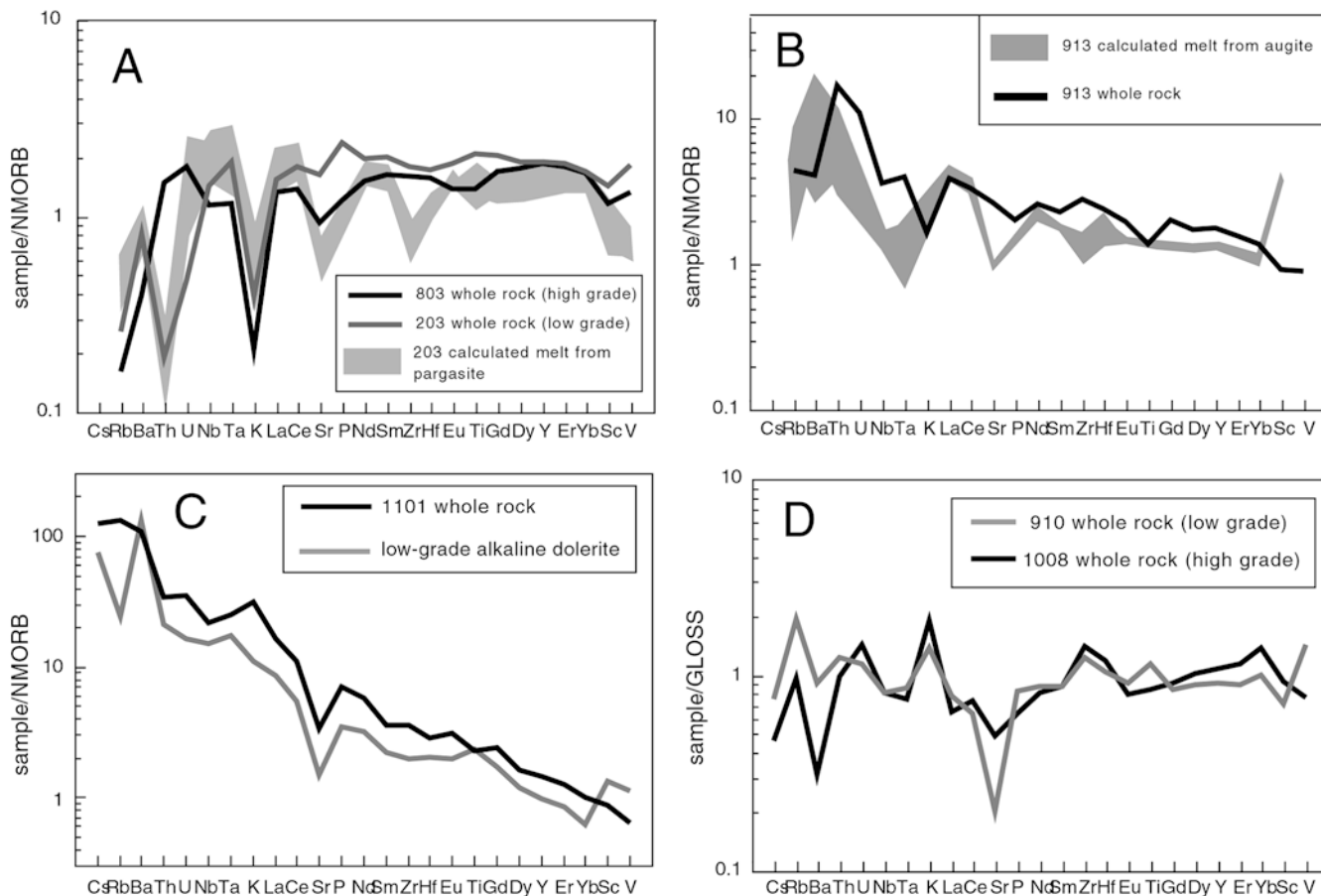| Sample no. Rock type	913 Lawsonite blueschist	203 Lawsonite blueschist	910 Lawsonite blueschist	1101 Garnet-epidote blueschist	803 Eclogite	1008 Quartz-mica schist	NIST 612 Glass standard
SiO_2	50.39	45.82	66.08	49.60	50.36	71.75	
TiO_2	1.83	2.21	0.80	2.89	1.90	0.54	
Al_2O_3	14.63	13.19	15.28	15.01	13.59	12.59	1.95
FeO	9.28	12.76	4.69	9.57	12.60	3.72	
MnO	0.11	0.26	0.09	0.37	0.21	0.11	
MgO	6.81	8.68	1.91	7.25	7.13	2.31	
CaO	8.33	9.16	1.21	5.61	9.23	1.75	11.85
Na_2O	2.65	3.43	3.86	3.75	3.50	0.61	
K_2O	0.12	0.03	2.77	2.29	0.02	3.87	
P_2O_5	0.23	0.20	0.17	0.85	0.14	0.13	
SO_3	0.10	1.05	0.01	0.00	0.41	0.09	
LOI	4.95	3.66	2.93	2.07	0.51	2.09	
Total	99.43	100.45	99.80	99.26	99.60	99.56	
Cu	44	nd	37	29	65	6	
Zn	89	nd	86	88	127	15	
Cr	132	nd	27	208	88	19	38
P	1,006	1,197	685	3,603	609	520	55
Sc	36.42	56.36	15.65	25.61	46.78	13.68	39
Ti	10,328	15,774	4,227	17,251	10,416	3,085	41
V	269	541	155	193	394	83.6	38
Co	30.1	59.4	9.19	35.5	46.5	12.12	35.5
Ni	65.1	72.8	20.3	84.7	55.1	26.5	38
Rb	2.47	0.14	108.9	74.11	0.09	55.04	32
Sr	240	146	66.0	303	83.2	159	78
Y	48.93	52.56	26.68	41.11	51.52	31.70	42
Zr	203	132	159	268	117	182	41
Nb	8.29	3.33	7.22	50.67	2.63	7.20	42
Mo	0.84	1.04	1.45	1.09	1.74	2.37	38.3
Cs	nd	nd	2.61	0.87	nd	1.60	41.5
Ba	25.56	5.09	700	691	2.48	240	38.5
La	9.77	3.80	22.56	40.96	3.30	18.48	36
Ce	25.04	13.20	36.26	82.2	10.23	42.19	38
Pr	3.72	2.50	5.64	10.02	1.92	5.14	38
Nd	18.77	14.30	23.58	42.04	11.00	21.61	35
Sm	6.01	5.24	5.02	9.51	4.26	5.03	38
Eu	1.99	1.87	1.19	3.18	1.40	1.03	36
Gd	7.43	7.40	4.40	9.01	6.15	4.76	38
Tb	1.26	1.33	0.72	1.30	1.14	0.77	36
Dy	7.78	8.60	4.42	7.33	7.92	5.03	36
Ho	1.63	1.85	0.89	1.37	1.73	1.07	38
Er	4.57	5.46	2.59	3.77	5.27	3.28	38.5
Tm	0.62	0.76	0.38	0.50	0.75	0.51	38
Yb	4.21	5.15	2.74	3.09	5.05	3.79	39
Lu	0.64	0.78	0.43	0.46	0.79	0.61	38
Hf	4.90	3.49	4.22	5.80	3.20	4.75	37
Ta	0.52	0.25	0.54	3.36	0.15	0.47	41
Pb	2.81	4.62	9.58	14.94	0.66	9.34	38.6
Th	2.00	0.02	8.36	4.13	0.18	6.72	37.8
U	0.52	0.02	1.90	1.67	0.08	2.37	37.4

See text for analytical details. nd, No data. Number of significant figures shown indicates level of precision

interference from inclusions was detected in many analyses and in all cases these interferences could be removed or avoided during data reduction. Minerals such as albite, chlorite and glaucophane have low trace element contents and are relatively uniform in composition, and hence only required a few LA-ICP-MS analyses. Minerals with relatively high trace-element compositions and/or long growth histories (lawsonite, titanite, garnet, epidote) often are complexly zoned and required a larger number of analyses.

Whole-rock geochemistry

The major and trace element compositions of all of the samples studied are presented in Table 2 and Fig. 3. Samples 203 and 803 have similar compositions indicating that they were formed from a common mafic protolith. Both have composition similar to normal mid ocean ridge basalt (NMORB; Fig. 3A), but have slight negative Eu and Sr anomalies, high Ti and Fe contents

and low LILE contents. These features are typical of mid ocean ridge gabbros. The presence of coarse Ti-rich pargasite and augite in 203 also supports a gabbroic protolith (Tribuzio et al. 2000). The trace element content of augite could not be measured due to partial replacement by metamorphic amphibole. However reliable analyses of Ti pargasite were obtained (Table 3 and Electronic Supplementary Table 1), allowing calculation of the original melt composition using amphibole/liquid partition coefficients (Fig. 3A). The calculated melt composition is very similar to the whole-rock composition of sample 203.

Samples 913 and 1101 are also mafic in composition although they contain higher concentrations of incompatible elements (Fig. 3B, C). 913 is relatively subalkaline but has enriched (E) MORB-like trace-element characteristics. As with sample 203, an estimate of the original trace-element melt composition of sample 913 is attainable using the composition of the original igneous augite (Table 3 and Electronic Supplementary Table 1) that is preserved in the rock and clinopyroxene/liquid partition coefficients. Again, calculated melt patterns (Fig. 3B) are similar to the bulk-rock composition for most elements. Garnet–bearing epidote blueschist sample 1101 is relatively low in CaO, but has high incompatible-element contents. These characteristics are typical of alkaline or ocean-island basalts (Sun and McDonough 1989; Wilson 1989). Furthermore 1101 is

Fig. 3A–D NMORB and GLOSS normalised trace-element variation diagrams of blueschist and eclogite-facies samples. Values for NMORB and GLOSS normalisation from Sun and McDonough (1989) and Plank and Langmuir (1998), respectively. **A** Whole-rock data for samples 203 and 803 and calculated melt data for 203. The calculated melt was determined using the composition of pargasite and partition coefficients from Rollinson (1993). **B** Whole-rock and calculated melt data for 913. Melt data were calculated using augite compositions and partition coefficients of White (2001). **C** Whole-rock data for sample 1101 and a low-grade alkaline dolerite. **D** Whole-rock data for pelitic samples 910 and 1008

Table 3 Representative major element mineral analyses. See text for details. Mineral abbreviations as in Table 1. Metamorphic grade abbreviations; *ig* igneous, *bl* blueschist, *ec* eclogite, *rg* retrograde

Mineral	aug	aug	parg	laws	laws	laws	tnt	tnt	tnt	tnt	gl	gl	gl	chl	chl	alb	gt core	gt rim	gt core	gt rim	hbl	omp	rt	apa	apa	phg	phg	phg	pump	zoi	zoi
Sample	913	203	203	913	910	203	1101	913	910	203	1101	803	913	913	910	910	1008	1008	803	803	1008	803	803	1101	1008	1008	1101	910	203	1101	803
mmph grade	ig	ig	ig	bl	bl	bl	bl	bl	bl	bl	bl	ec	bl	bl	bl	bl	ec	ec	ec	ec	ec	ec	ec	bl	ec	ec	bl	bl	rg	bl	ec
SiO_2	52.16	52.46	45.67	38.34	38.41	38.09	30.34	31.49	31.29	30.11	57.48	58.29	57.36	27.58	25.13	69.11	36.88	37.55	37.26	38.03	46.18	55.62				48.23	50.3	50.7	36.95	37.54	38.05
TiO_2	0.51	0.29	1.88	0.59	0.13	0.26	39.02	36.41	37.35	39.05	0.03	0.07	0.23	0			0.05	0.08	0.16	0.05	0.5	0.03	100.11			0.9	0.32	0.15	2.92	0.09	0.12
Al_2O_3	3.84	2.03	10.26	31.41	31.82	31.82	1.35	2.23	2.3	1.04	10.24	10.59	10.71	18.78	19.36	19.53	20.72	21.17	20.69	21.46	12.26	9.79	0.10			27.3	26.25	26.52	24.04	25.13	27.84
Fe_2O_3				0.56	0.20	0.53	0.29	1.21	0.71	0.43													0.09						3.11	10.56	6.82
FeO	9.38	9.67	13.88								9.39	8.36	14.95	22.88	33.3		24.75	26.27	24.3	27.91	13.73	5.34		0.06	0.14	3.41	3	3.69	1.14	0.35	0.18
MnO	0.15	0.24	0.49	0.00	0.12	0.03	0.04	0	0.02	0.11	0.02	0	0.09	0.16	0.57		7.75	1.99	4.86	0.17	0	0.07						0.02	0.04		
MgO	15.21	13.13	11.9	0.07	0.02	0.01					11.85	11.86	7.52	18.03	10.46		2.14	3.62	0.82	2.87	11.46	8.3			0.04	3.12	3.64	2.72	3.11	0.10	0.15
CaO	17.2	21.56	10.91	17.68	16.96	17.28	28.49	28.36	27.91	28.22	1.65	0.84	0.56	0	0.08	0.00	8.55	8.98	11.23	9.71	9.31	13.78		54.97	54.04	0	0.06	0.44	22.05	22.92	23.83
Na_2O	1.58	0.47	2.87	0.11							6.77	7.32	7.64	0.21		11.72	0.09	0.16	0	0.05	3.56	6.83				0.75	0.5		0.31	0.09	0.00
K_2O	0.47		1.46								0.04	0		0.21		0.00		0.16			0.6					9.94	10.81	10.47			
P_2O_5			0.02							0	0.04	0				0.00	0.09	0.05	0				0.09	40.54	39.67						
H_2O (calc)			2.04	11.46	11.38	11.39	0.35	0.97	0.77	0.28	2.18	2.19	2.16	11.54	11.01						2.05					4.38	4.44	4.44	5.53	1.88	1.91
Total	100.03	99.85	99.92	100.22	99.04	99.42	99.88	100.67	100.35	99.24	99.65	99.52	101.22	99.18	99.91	100.36	100.93	99.82	99.32	100.25	99.65	99.76	100.35	95.57	93.89	98.03	99.15	99.36	99.17	98.66	98.90
Oxygens used	6	6	23	8	8	8	5	5	5	5	23	23	23	28	28	8	12	12	12	12	23	6	2	12.5	12.5	22	22	22	12.5	12.5	12.5
Si	1.91	1.96	6.68	2.01	2.02	2.01	0.99	1.03	1.02	0.99	7.86	7.94	7.94	5.73	5.48	3.00	2.95	2.97	3.00	3.00	6.70	1.98				6.61	6.79	6.85	3.00	3.00	2.99
Ti	0.01	0.01	0.21	0.02	0.01	0.01	0.96	0.89	0.92	0.97	0.00	0.01	0.02	0.00			0.00	0.00	0.01	0.00	0.05	0.00	1.00			0.09	0.03	0.02	0.18	0.01	0.01
Al	0.17	0.09	1.77	1.94	1.98	1.97	0.05	0.09	0.09	0.04	1.65	1.70	1.75	4.60	4.97	1.00	1.95	1.98	1.96	1.99	2.10	0.41	0.00			4.41	4.18	4.22	2.30	2.36	2.58
Fe^{3+}	0.10	0.00	0.23	0.02	0.01	0.02	0.01	0.03	0.02	0.01	0.35	0.24	0.11								0.38	0.06	0.00						0.19	0.63	0.40
Fe^{2+}	0.19	0.30	1.46								0.73	0.71	1.62	3.98	6.07		1.65	1.74	1.64	1.84	1.29	0.10				0.39	0.34	0.42			
Mn	0.00	0.01	0.06	0.00	0.01	0.00	0.00	0.00	0.00	0.00	0.00	0.00	0.01	0.03	0.11		0.52	0.13	0.33	0.01	0.00	0.00		0.00	0.00	0.00	0.00	0.00	0.08	0.02	0.01
Mg	0.83	0.73	2.59	0.01	0.00	0.00					2.41	2.41	1.55	5.59	3.40		0.25	0.43	0.10	0.34	2.48	0.44		0.00	0.00	0.64	0.73	0.55	0.38	0.01	0.02
Ca	0.67	0.86	1.71	0.99	0.96	0.97	1.00	0.99	0.98	1.00	0.24	0.12	0.08	0.00	0.02	0.00	0.73	0.76	0.97	0.82	1.45	0.53		5.09	5.04	0.00	0.01	0.00	1.92	1.96	2.01
Na	0.11	0.03	0.81	0.01							1.79	1.93	2.05	0.08		0.99	0.01	0.02	0.00	0.01	1.00	0.47		0.00	0.01	0.20	0.13	0.12	0.05	0.01	0.00
K	0.00										0.01	0.00	0.00			0.00					0.11					1.74	1.86	1.81			
P			0.00																					2.96	2.98						
Cation sum	4.00	4.00	15.53	5.00	4.98	4.99	3.02	3.03	3.02	3.02	15.04	15.05	15.13	20.01	20.04	4.99	8.08	8.04	8.01	8.01	15.56	4.00	1.00	8.05	8.03	14.07	14.08	13.98	8.10	8.01	8.01

very similar in composition to a low-grade alkaline dolerite (Fig. 3C) that outcrops to the west of (below) the lawsonite isograd (see Fig. 1).

The trace-element composition of the pelitic samples 910 and 1008 are compared with the calculated average global subducting sediment (GLOSS; Plank and Langmuir 1998) in Fig. 3D. The distinct Sr anomaly is due to the incorporation of a Sr-rich carbonate component in GLOSS (Plank and Langmuir 1998). Despite this, both of the pelite samples are similar to GLOSS and therefore are excellent analogues of subducted sedimentary material. Moreover, the pelites are very similar in composition, indicating they were originally part of the same sedimentary sequence.

Loss on ignition (LOI) values for all samples compare closely to bulk-rock water contents calculated using mineral compositions and modes (Table 1), indicating that water comprises most of the volatile component of the samples. As the lawsonite blueschists have higher water contents than their higher-grade counterparts, metamorphism is most likely to be accompanied by devolatilisation.

Mineral chemistry

Major element mineral compositions are presented in Tables 3 and 4. For amphibole and clinopyroxene,

ferric and ferrous iron contents were calculated on the basis of charge balance. All iron was assumed to be Fe^{3+} for lawsonite, pumpellyite, rutile, titanite and zoisite and Fe^{2+} for mica, garnet, chlorite, apatite and allanite. The water content of hydrous minerals was calculated assuming stoichiometry. The major-element compositions of metamorphic minerals are typical of blueschist and eclogite-facies rocks. Lawsonite and albite deviate very little from their ideal formula. Titanites often contain small amounts of Al and Fe. Sodic amphibole varies from Fe-rich glaucophane in the lawsonite blueschists to glaucophane in the higher-grade rocks. Phengite has ~3.3 Si per-formula-unit (pfu) in samples 1101 and 1008 and ~3.4 Si pfu for 910.

Garnet in the higher-grade rocks is dominantly almandine in composition, but does have significant zoning from spessartine-rich cores to spessartine-poor rims. These compositions are consistent with growth of garnet during prograde metamorphism. Omphacite in 803 contains approximately 0.4 mole of jadeite and 0.06 mole of aegerine. Zoisite in all samples has between 0.1–0.2 moles of pistacite and the hornblende in 1008 is barroisitic.

There is very little major-element chemical variation in most of the minerals examined in this study. In contrast, the trace element characteristics of the minerals can be highly complex and therefore requires in-depth

Table 4 Major element composition of allanite from samples 913 and 1008. See text for analytical details

Sample	913-1 core	913-2 core	913-3 core	913-4 core	913-5 rim	1008-1	1008-2	1008-3
SiO_2	33.97	31.66	32.20	32.06	35.72	38.31	37.98	36.28
Al_2O_3	21.66	20.43	21.09	21.07	23.10	25.57	25.13	23.74
FeO	10.86	10.98	10.56	10.90	11.90	7.96	8.05	8.57
MnO	0.21	0.19	0.19	0.25	0.28	0.10	0.10	0.09
MgO	0.07	0.06	0.06	0.07	0.04	0.26	0.30	0.26
CaO	14.32	13.79	14.82	14.85	21.18	21.36	21.34	20.57
SrO	2.22	2.33	2.66	4.00	0.36	0.56	0.59	0.68
Y_2O_3	0.05	0.03	0.08	0.08	0.13	0.17	0.15	0.05
La_2O_3	2.14	2.26	1.77	1.58	0.49	0.58	0.67	0.63
Ce_2O_3	5.52	5.75	4.71	3.74	1.17	1.30	1.51	1.62
Pr_2O_3	0.83	0.85	0.73	0.55	0.16	0.09	0.23	0.20
Nd_2O_3	3.68	3.78	3.32	2.67	0.77	0.60	0.72	0.76
Sm_2O_3	0.55	0.37	0.57	0.37	0.15	0.15	0.16	0.23
Gd_2O_3	0.21	0.04	0.10	0.06	0.12	0.08	0.13	0.11
ThO_2	0.45	0.21	0.61	0.68	0.14	0.34	0.25	0.44
H_2O (calc)	1.67	1.58	1.61	1.61	1.76	1.85	1.83	1.76
Total	98.43	94.31	95.06	94.54	97.46	99.27	99.15	96.00
Oxygens	12.5	12.5	12.5	12.5	12.5	12.5	12.5	12.5
Si	3.04	2.99	2.99	2.98	3.04	3.11	3.10	3.09
Al	2.29	2.28	2.31	2.31	2.31	2.45	2.42	2.38
Fe	0.81	0.87	0.82	0.85	0.85	0.54	0.55	0.61
Mn	0.02	0.01	0.01	0.02	0.02	0.01	0.01	0.01
Mg	0.01	0.01	0.01	0.01	0.00	0.03	0.04	0.03
Ca	1.38	1.40	1.48	1.48	1.93	1.86	1.87	1.88
Sr	0.12	0.13	0.14	0.22	0.02	0.03	0.03	0.03
Y	0.00	0.00	0.00	0.00	0.01	0.01	0.01	0.00
La	0.07	0.08	0.06	0.05	0.02	0.02	0.02	0.02
Ce	0.18	0.20	0.16	0.13	0.04	0.04	0.04	0.05
Pr	0.03	0.03	0.02	0.02	0.01	0.00	0.01	0.01
Nd	0.12	0.13	0.11	0.09	0.02	0.02	0.02	0.02
Sm	0.02	0.01	0.02	0.01	0.00	0.00	0.00	0.01
Gd	0.01	0.00	0.00	0.00	0.00	0.00	0.00	0.00
Th	0.01	0.00	0.01	0.01	0.00	0.01	0.00	0.01
Cation sum	8.11	8.14	8.14	8.18	8.27	8.14	8.13	8.15
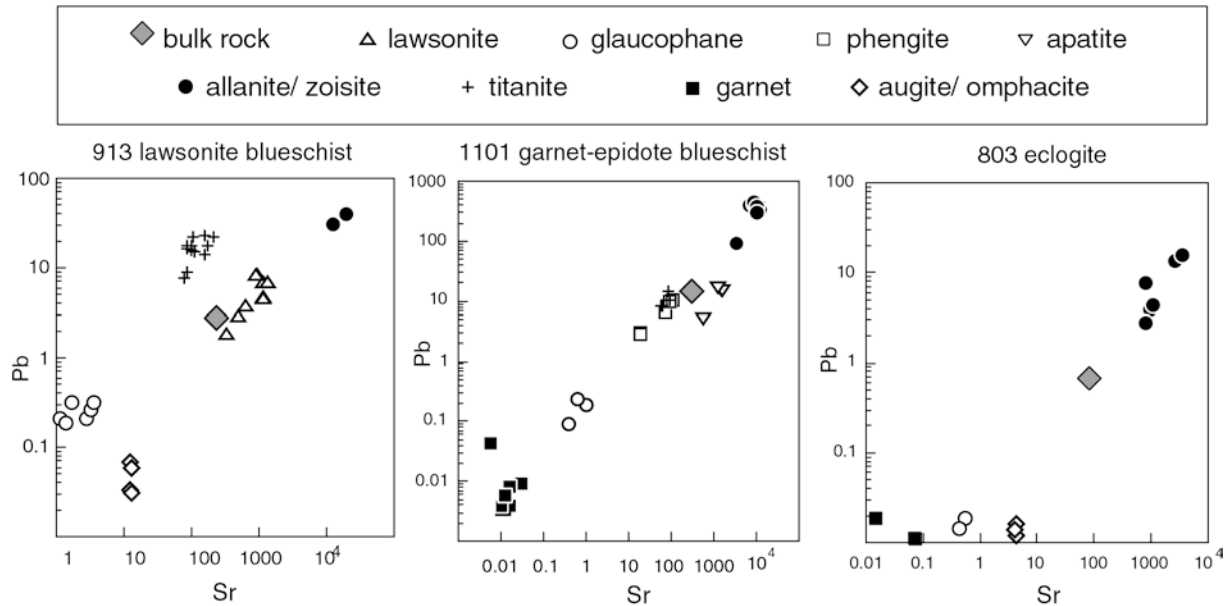
**Fig. 4** Sr and Pb compositions for bulk-rock and minerals of mafic samples 913, 1101 and 803

analysis. Strontium and Pb compositions from three mafic samples, and mineral REE patterns for all samples are presented in Figures 4 and 5 respectively. Due to the similar charge and ionic radii of Sr (2+; 132 pm) and Pb (2+; 133 pm), the concentration of these elements directly correlate in the minerals (Fig. 4). In the blueschist-facies samples, albite, glaucophane and chlorite contain low concentrations of most trace elements (Figs. 4 and 5; Electronic Supplementary Table 1). Lawsonite in all samples has very high Sr concentrations. In the mafic samples, lawsonite has appreciable Th and Pb and low HFSE and U contents. REE patterns for lawsonite may be flat, HREE-depleted or LREE-enriched and range from 1–100 times chondritic values. Lawsonite in 910 is a minor phase but contains high concentrations of Th, U and Pb. REE patterns are between 10–1,000 times chondrite and are slightly LREE enriched, reflecting the bulk-rock REE content. Calcite in samples 910 also has very high Sr contents, but contains very low levels of other investigated elements.

Titanite in all of the blueschist samples may contain high concentrations of REE, HSFE, Sr, Ba, Th, U and Pb (Figs. 4 and 5). However, there are large variations in the trace element compositions of grains within and between samples. We suggest that these variations reflect the timing of titanite growth with respect to other trace element-rich minerals and variations in bulk-rock trace element contents. Most titanite grains in sample 203 have strongly LREE-depleted REE patterns and low concentrations of Zr and Hf. These grains are interpreted as crystallising from a LREE-depleted matrix after lawsonite formation and in the presence of zircon. One grain has a flat REE pattern with a positive Eu anomaly and relatively low Sr and high Zr and Hf contents. We suggest this grain formed prior to meta-

morphism by hydrothermal alteration of igneous-derived Fe-Ti oxides or pargasite and plagioclase. Sample 913 contains titanite with relatively flat REE patterns, and variable U, Th, Zr and Hf contents indicating crystallisation occurred with or without zircon, but prior to lawsonite or allanite growth. Titanite in sample 910 is similar to 913 except it has higher Nb, Pb, Th and U contents and convex-up REE patterns. Titanite in sample 1101 is enriched in Nb and Ta but has very low Ba, Zr and Hf contents. REE patterns are consistently LREE depleted, but absolute REE concentrations vary considerably. These features are consistent with retrograde formation of titanite from rutile in the presence of zircon, phengite and epidote.

The epidote-group minerals have by far the largest variations in composition. Despite the application of high-precision analytical techniques, major-element allanite analyses often gave low totals and poor stoichiometry (Table 4). We attribute this to the presence of unaccounted Fe^{3+} and difficulties associated with measuring REE. Nonetheless, determination of REEs, Y, Sr and Th by WDS microprobe compares well with LA ICP-MS analyses (samples 913 in Fig. 5). Allanite is a trace mineral in sample 913 and contains very high concentrations of light to middle REE, (~10 wt%), Sr (up to 4 wt%) and Th (up to 1 wt%). Significant amounts of Ba, U and Pb are also present. WDS microprobe analyses reveal that the thin zoisite rims around allanite also host high concentrations of these elements. Allanite in samples 1008 and 1101 also has high REE, Th, U, Pb and Sr but low Ba contents. In both samples, there is a progressive decrease in these elements to zoisite which is consistent with the zoning seen under backscatter SEM images (Fig. 2). The cause of the positive Eu anomaly in zoisite is uncertain, but may be related to late-stage breakdown of plagioclase. Epidote in sample 803 is zoisite with relatively flat REE patterns. Nonetheless, it also contains high but variable concentration of REE, Sr, Pb, Th and U.

214

Fig. 5 Chondite-normalised
rare-earth element plots of
metamorphic minerals.
Normalising values from
Taylor and McLennan (1985)
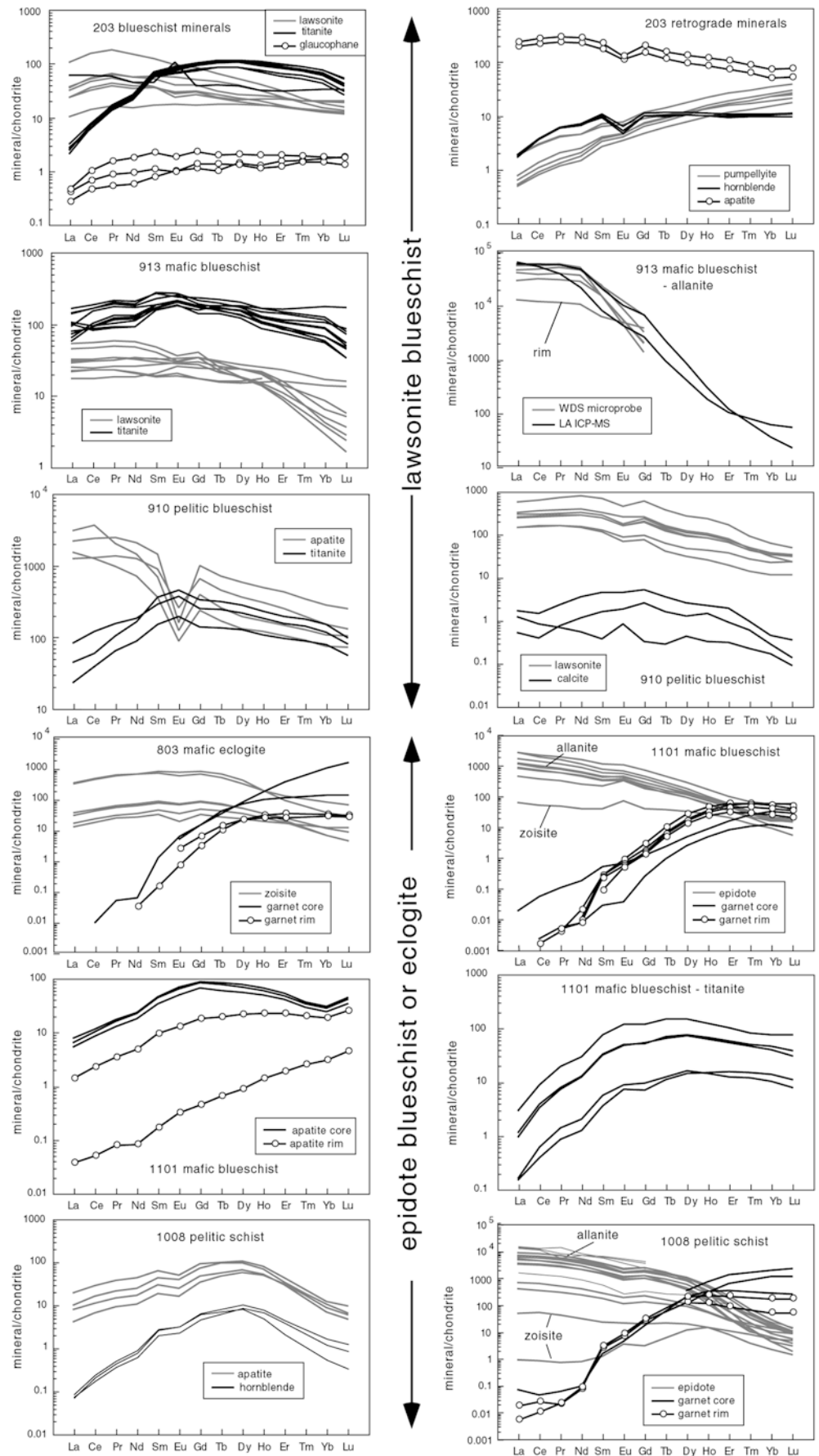
Apatite hosts significant amounts of Sr, Pb and REE, but also has considerable compositional variation within and between samples. Metamorphic apatite in samples 1101 and 1008 has slightly convex to LREE-depleted REE patterns and have notable variations in LREE content. There is a decrease in LREE and Sr concentration from the core to rim of apatite grains from 1101. In sample 910, apatite has LREE-enriched REE patterns with a large negative Eu anomaly and is unlike the metamorphic apatites from samples 1101 and 1008. Apatite in sample 910 is similar in composition to apatite from granitic rocks (Belousova et al. 2001) and hence is interpreted to be detrital grains that have resisted metamorphic alteration.

Preservation of zoning in garnet is typical of high-pressure metamorphic rocks, although trace element zoning has rarely been reported (Rubatto 2002). Garnet from all of the high-grade samples has low Sr and Pb contents (Fig. 4) and steep REE patterns with high HREE/LREE ratios (Fig. 5). For samples 803 and 1008, core to rim zoning is manifest as a relative depletion in HREE. Zoning is less pronounced in sample 1101, although the rims have a slight relative enrichment of MREE. These rim compositions are suggested to have formed during the high-pressure reactions including breakdown of MREE-bearing titanite to form REE-poor rutile. Omphacite and hornblende are also important constitutes of eclogite-facies rocks, yet in samples 803 and 1008 these minerals contain low concentrations of all key trace elements. Rutile and phengite also have very low REE contents. Nonetheless, rutile is the principle host of Nb and Ta, while phengite contains very high concentrations of Cs, Rb and Ba, and may contain high concentrations of Sr and Pb (Fig. 4).

Retrogression is insignificant in all samples except 203, which has a well-developed greenschist-facies assemblage formed from the breakdown of blueschist-facies minerals. Trace element analysis of these minerals allows for the evaluation of elemental distribution during transformation from blueschist to greenschist. The major phases formed from lawsonite and glaucophane breakdown are pumpellyite, albite and hornblende. To our knowledge we present the first trace-element analysis of pumpellyite. Pumpellyite clearly replaces lawsonite, but is relatively depleted in LREE and most other trace elements. Hornblende and albite also have low trace element contents. In contrast, apatite is only a minor phase of the greenschist-facies assemblage, but contains elevated REE and Sr concentrations. Therefore, apatite may balance the trace element budget of lawsonite breakdown.

Whole-rock elemental budgets

The distribution or budget of trace elements among the mineral inventory of all six samples was calculated using the relative proportions of minerals (Table 1) and the average major and trace-element composition of the minerals. Mineral modes were determined by thin section observation and mass balance using the bulk-rock major-element chemistry and total major-element mineral chemistry. The calculated trace-element budgets are presented graphically in Fig. 6. Precise budgeting of many trace-elements in the lawsonite blueschists is difficult due to their complex mineralogy and fine grainsize. Nonetheless, the distribution of most trace elements is well constrained with a few notable exceptions. Poor element budgeting arises for one of the following reasons: (1) inaccurate average mineral compositions due to heterogeneous trace-element distribution and zoning in minerals such as epidote, titanite and garnet or (2) lack of data for trace-element-rich minor phases such as phengite and zircon. Zr and Hf are poorly constrained in all samples, and are expected to be dominantly accommodated by zircon, which has not been analysed. This is consistent with previous work which has shown that zircon hosts over 90% of the Zr and Hf in eclogite-facies rocks (Hermann 2002; Rubatto and Hermann 2003). Pre-metamorphic phases such as pargasite, augite, and apatite can retain large amounts of trace elements (up to 25% in sample 203), effectively limiting element availability during metamorphism. Nonetheless, it is clear that lawsonite, titanite, allanite and phengite are the most important metamorphic minerals for hosting trace elements in these samples. Chlorite, glaucophane and albite comprise the bulk of the blueschist-facies assemblages, but collectively account for less than 5% of their trace-element stocks. Lawsonite from the mafic blueschists is host to over 90% of the Sr, ~30% of the LREE and significant proportions of Th and other REE. Allanite in sample 913 is the major host for LREE and Th. Titanite in all blueschist samples contains the majority of the Nb, Ta and Ti, and up to 50% of M-HREE. Pb is hosted primarily by lawsonite and titanite in sample 913, and is most likely hosted by sulfides in sample 203, although we lack trace-element data for the sulfides. The trace-element distribution budgets for sample 910 are very poorly constrained, particularly for LREE, HREE, Pb, Th, and U. Unrecognised trace minerals such as allanite, monazite, xenotime or HREE-rich titanite may account for these discrepancies. Cs, Rb, Ba, and Sr are better constrained, and are hosted by phengite and calcite respectively. Rb and Ba are also expected to be hosted by trace phengite in sample 913. Sample 203 lacks a mica phase, so Rb and Ba are distributed among the entire mineral inventory.

Overall, the trace element budgets for the higher-grade rocks are more precisely constrained as they have experienced complete recrystallisation and limited retrogression. In the mafic rocks (803, 1101), epidote is the host for over 95% of the U, Th, Pb, Sr and light to middle REE, regardless of the type (allanite or zoisite) or amount of epidote in the rock. Epidote in sample 1008 also contains most of the LREE but is only host to 25% of the Pb and 50% of the Sr. Phengite in the alkaline rocks accounts for nearly 100% of the Cs, Rb and Ba and significant proportions of Sr and Pb. Titanite and/or

Fig. 6 Trace element distribution or budget for blueschist and eclogite-facies samples. See text for details
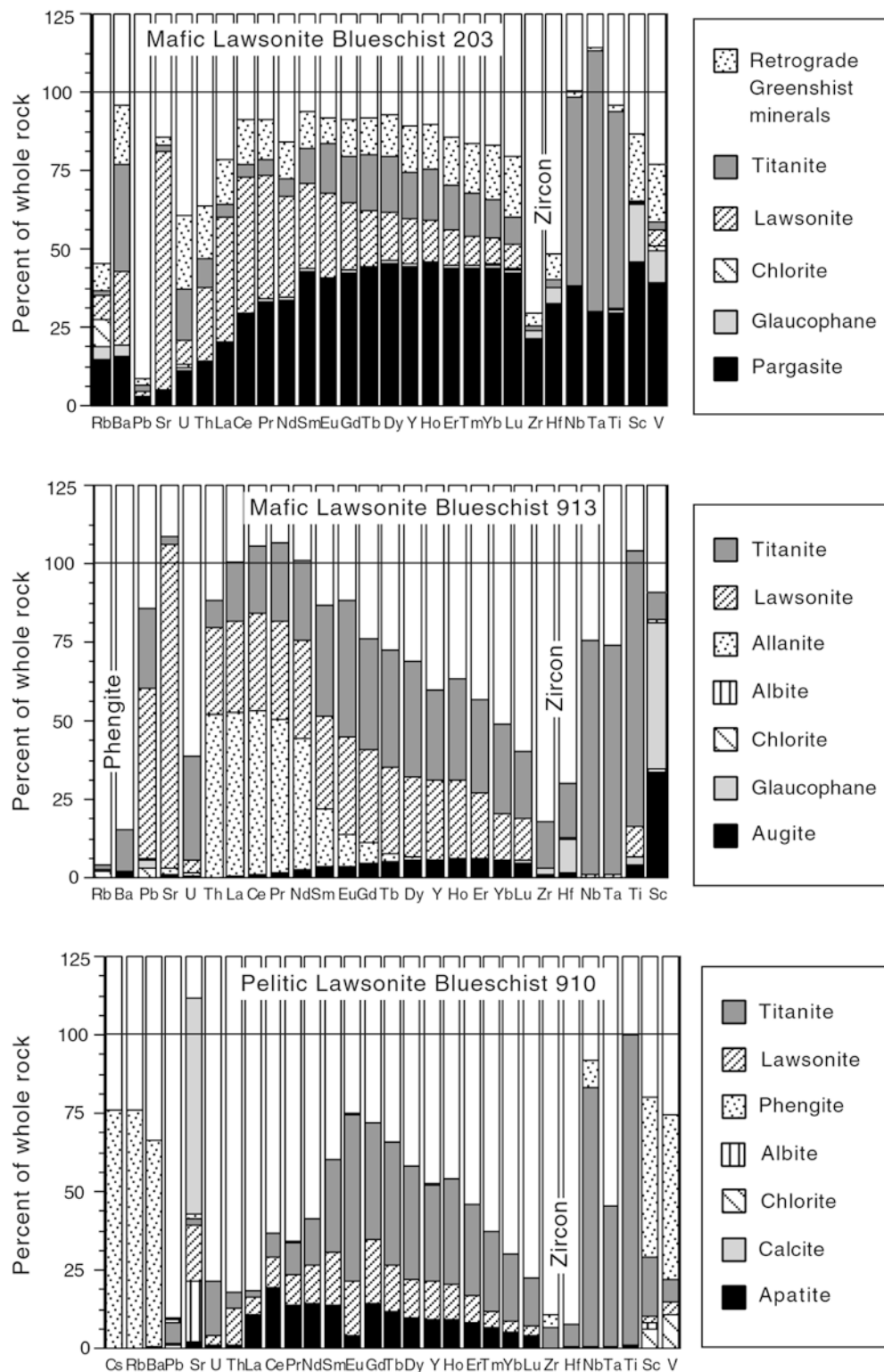

rutile contains over 90% of the Nb and Ta and garnet hosts 30–70% of the HREE. The transition elements (Sc and V) are distributed among the entire mineral inventory in all of the samples. With the exception of these elements, amphibole, apatite and omphacite collectively account for less than 3% of the trace-element budgets of these rocks.

Discussion

Trace element partitioning

Knowledge of the equilibrium partitioning of elements among coexisting phases is useful for predicting the

Fig. 6 (Contd.)
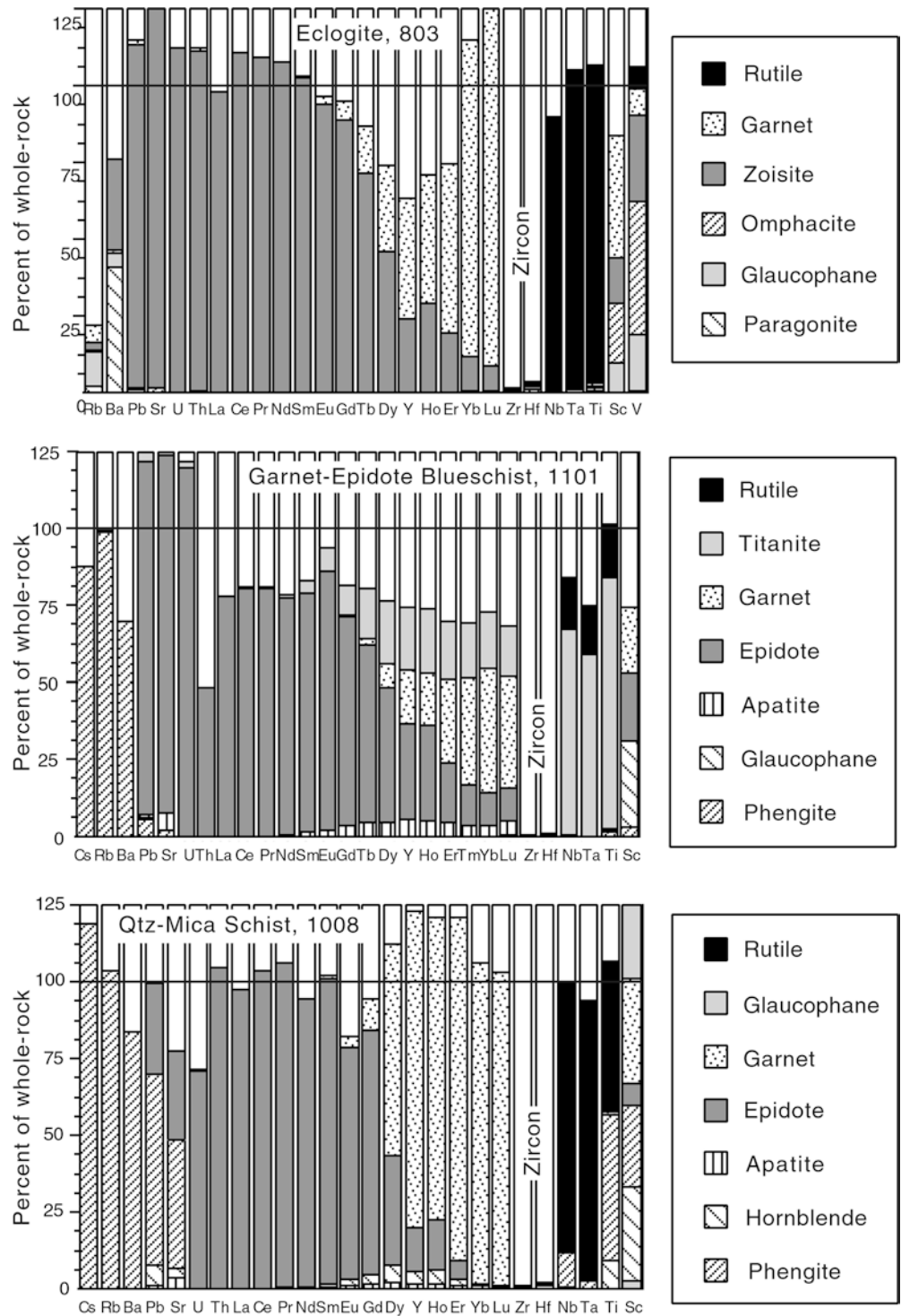
distribution of trace element in lithologies of the subducted slab and may be used to determine subduction-zone fluid compositions through indirect calculations of mineral/fluid partitioning. The distribution of trace elements between lawsonite and titanite varies considerably between samples (Fig. 5), indicating that these phases are not in equilibrium in all cases. We suggest that the low temperatures of metamorphism and the lack of deformation suppress the attainment of equilibrium and allow for the persistence of igneous and detrital mineral grains. Our results are in agreement with several previous studies that demonstrated significant trace element disequilibrium between minerals in blueschist and eclogite-facies rocks (Thöni and Jagoutz 1992; Getty and Selverstone 1994; Messiga et al. 1995; Zack et al. 2002). This is also the case for the lawsonite blueschist samples studied here. Growth of metamorphic minerals is likely to occur continuously over a range of P and T

Table 5 Approximate mineral-mineral partition coefficients for selected trace elements

Sample	Minerals	Sr	Pb	Ce	Y	Yb	U	Th	Zr	Nb	Ba
1101	gt/gl	0.03	0.03	3	~2,000	~2,000	0.5	1.5	~20	0.2	0.01
1101	ep/gt	10^5–10^6	10^4–10^6	$>3\times10^5$	1–2	0.2–0.4	5,000–5×10^4	50–15,000	1–3	–	1,000–5,000
1101	ph/gt	10^3–10^4	300–1,500	~1	~0.001	<0.001	0.5	–	0.01–0.03	500	10^5–10^6
803	ep/omp	200–800	200–1,200	>5,000	300–3,000	500–3,000	>10	>10	5–10	<1	50–150
803	ep/gt	10^4–10^6	100–10^3	1,500–4×10^4	0.2–5	0.1–1	>100	>50	~5	~1	>50
1008	ep/amp	20–80	20–30	5–3,000	5–10	5–20	50–5,000	100–10^6	~0.5	<0.05	<0.05
1008	gt/amp	0.001	.001	0.05–0.2	20–50	50–200	1–5	~2	0.1–1	0.005	0.01
1008	ap/amp	20–30	4	30–150	10–15	5–10	50–100	4–30	0.01	0.002–0.02	0.02–0.05
1008	ph/amp	3	2	0.05	0.003	0.01	0.7	2	0.05	4	350
203	ap/pump	15–25	2–4	80–350	6–10	2–5	100–150	50–100	0.5–3	0.05–0.2	0.05–0.1

conditions, with new phases in disequilibrium with surrounding grains in many cases. We expect that rocks of the subducting slab will experience similar disequilibrium conditions, and preservation of relict igneous and detrital minerals to depths equivalent to the blueschist to eclogite transition (~70–150 km). These conditions need to be considered when modelling the release of fluid or trace elements from the slab.

In the higher-grade samples (803, 1008, 1101) where complete recrystallisation has occurred, many phases are in textural and chemical equilibrium and may be used to calculate approximate trace-element partition coefficients (Ds). Precise evaluation of Ds is difficult as many phases (e.g. garnet, zoisite/allanite) have long growth histories and are strongly zoned. Nonetheless, we have calculated approximate trace element Ds for a range of mineral pairs using rim compositions that are interpreted to be in equilibrium (Table 5). The strong affinities of epidote for Sr, Pb, Th, U and REE, phengite for LILE and garnet for HREE is reflected in the estimated D values. These Ds are very similar to corresponding Ds calculated from experiments (Brenan et al. 1995) and natural rocks formed under similar P and T conditions (Sorenson and Grossman 1989; Messiga et al. 1995; Sassi et al. 2000; Zack et al. 2002). The retrograde minerals pumpellyite and apatite in sample 203 are also suggested to have attained complete trace-element equilibrium. Both minerals pseudomorph lawsonite, contain inclusions of each other and have relatively uniform trace-element compositions. Apatite/pumpellyite Ds for selected trace elements are listed in Table 5.

Dehydration during prograde metamorphism

The variation in water contents of the mafic samples suggests that approximately 3–4 wt% water is liberated during the transition from lawsonite blueschist (4–5 wt% water) to eclogite (<1 wt% water). The majority of this fluid would be derived from the breakdown of lawsonite and chlorite. This is consistent with calculated budgets for water release from blueschist-facies mafic rocks in subducting slabs (Peacock 1993; Schmidt and Poli 1998). Lawsonite dehydration results in a relative volume increase, causing hydrofracturing of the rock (Nishiyama, 1989) and rapid fluid release. Hydrofracturing in the slab is likely to be a major cause of intermediate-depth intraslab earthquakes (Davies 1999). As the depth of most of these earthquakes (Kirby et al. 1996) correlates with the expected depth of lawsonite dehydration in the subducting slab (Peacock 1996; Kincaid and Sacks 1997; Schmidt and Poli 1998), we expect that lawsonite dehydration is a major cause of intraslab earthquakes.

The water content of the pelitic samples indicates that less than 1 wt% of water is released during the transition from blueschist to eclogite-facies in subducted sediments. However, eclogite-facies pelitic rocks may retain over 2 wt% water (Table 1). Minerals such as lawsonite and chlorite collectively comprise only minor amounts of these rocks and therefore contribute relatively little to the water budgets. Phengite is the most important water-bearing phase but is stable to very high pressures and temperatures (Domanik and Holloway 1996) effectively inhibiting fluid release (Hermann and Green 2001).

Liberation of trace elements

Studies of high-pressure veins and fluid inclusions from high-P, low-T terranes indicates that there is significant element mobility in the slab under eclogite-facies conditions (Philippot and Selverstone 1991; Becker et al. 1999; Xiao et al. 2000; Scambelluri and Philippot 2001). However, the mechanisms of element release from these rocks is not clear. It is often assumed that fluid-mobile elements (e.g. LILE) are released to fluids during metamorphic breakdown of trace-element-rich minerals. Alternatively, elements may be liberated without mineral breakdown through fluid/mineral partitioning in zones of high fluid-rock interaction (Sorenson et al. 1997). Here and elsewhere (Tribuzio et al. 1996; Sorenson et al. 1997; Arculus et al. 1999; Sassi et al. 2000; Hermann 2002; Rubatto 2002; Zack et al. 2002) a range of important trace element-hosting minerals are identified, but almost nothing is known of the fate of the trace elements during mineral breakdown. Comparison between the New Caledonian samples of similar protolith reveals that the chemical composition of these rocks

has not changed significantly during the transformation through lawsonite blueschist-facies to eclogite-facies assemblages (Fig. 3). This is consistent with previous work on trace element distribution in high-pressure rocks (Shatsky et al. 1990; Tribuzio et al. 1996) and indicates that subducting slabs do not experience extensive loss of trace elements due to the breakdown of hydrous minerals up to eclogite facies. We are able to evaluate whether or not trace elements are liberated by mineral breakdown reactions by determining the trace-element hosts in a range of low and high-grade metamorphic rocks.

The major hosts for trace elements are lawsonite (REE, Pb, Sr), titanite (REE, Nb, Ta), and allanite (LREE, U, Th) under lawsonite blueschist-facies conditions and epidote (REE, Sr, Th, U, Pb), garnet (HREE) and rutile (Nb, Ta) under eclogite-facies conditions. At all metamorphic grades, phengite and zircon contain almost all of the LILE and Zr and Hf respectively. Minerals, such as chlorite, albite, amphibole and omphacite often make up the bulk of these metamorphic assemblages but contribute very little to the whole-rock trace-element budgets. Phengite, apatite, allanite and zircon are stable in mafic and pelitic rocks from lawsonite blueschist-facies to conditions in excess of 4.0 GPa and 800 °C (Domanik and Holloway 1996; Hermann 2002). This limits the available mass of trace elements that may be liberated by mineral breakdown at sub arc levels (~3.0 GPa). Furthermore, these minerals may become included in other phases or overgrown by a later generation of a similar mineral (e.g. zoisite armouring allanite; Fig. 3D, E), effectively isolating them from dehydration processes and fluid alteration. This process also limits the availability of trace elements for further mineral growth and in many cases accounts for the trace element zoning observed in minerals such as garnet, epidote and apatite.

Titanite and lawsonite contain appreciable levels of U, Th, Pb, Sr and REE, which potentially may be mobilised during mineral breakdown. The breakdown of lawsonite and titanite produces zoisite, garnet and rutile at pressures below 3 GPa (Itaya et al. 1985; Poli and Schmidt 1995; Frost et al. 2001). This is consistent with the change in mineral assemblages observed in the blueschist and eclogite samples studied here. All of the trace elements released by lawsonite and titanite decomposition may be redistributed into zoisite/allanite, garnet and rutile. Especially interesting are the fluid-mobile elements Sr and Pb, which are incorporated mainly in titanite and lawsonite at lawsonite blueschist conditions (Fig. 4). During prograde metamorphism and dehydration to eclogite-facies conditions, significant amounts of Pb and Sr are retained into newly formed zoisite/allanite (Fig. 4). Hence, the Pb and Sr contents of the fluid are not likely to increase drastically due to the breakdown of Pb and Sr-rich phases. We predict that garnet and zoisite/allanite will similarly incorporate the relatively small amount of trace elements liberated by

amphibole dehydration at ~2.5 GPa (Poli and Schmidt 1995).

Evaluation of trace element redistribution during mineral reactions at pressures over 3 GPa is made by combining our data with experimentally-determined phase equilibria at high pressures. For mafic to pelitic compositions, pure zoisite breaks down to garnet, kyanite and quartz at ~3 GPa (Poli and Schmidt 1995). However, the high trace element content of zoisite strongly affects stability relations and reaction products. Hermann (2002) has shown that REE-bearing zoisite in crustal rocks progressively transforms to clinopyroxene, kyanite and allanite between 2.0–3.5 GPa and 650–850 °C. Water is released during this reaction but the mineral phases retain all of the trace elements.

Allanite is stable to over 4.5 GPa and 1050 °C in a range of crustal rock-types (Hermann and Green 2001; Hermann 2002). We predict that the high-pressure dehydration of lawsonite will also produce accessory allanite. This is represented by the following reaction, modified from Poli and Schmidt (2002):

$$\text{Lawsonite} + \text{Diopside} + \text{Garnet}(\text{gr}_{20}\text{py}_{80})$$
$$\rightarrow \text{Garnet}(\text{gr}_{40}\text{py}_{60}) + \text{Allanite} + \text{Fluid}$$
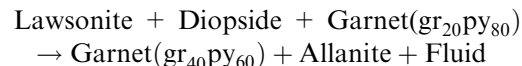
In this case, even trace amounts of allanite may sequester all of the garnet-incompatible elements liberated by lawsonite. Garnet and allanite may also be the product of the breakdown of titanite at high pressures, but we note that aluminous titanite is stable at very high pressures (> 3 GPa) in some rock-types (Carswell et al. 1996; Troitzsch and Ellis 2002).

In summary, we find no evidence to support a simple coupled release of fluid and trace elements by mineral breakdown reactions over a large range of P and T conditions. Instead, the investigated trace elements are redistributed into newly stabilised mineral phases. Evidence supporting the formation of trace element-rich phases during mineral breakdown includes the multiply-zoned epidote grains in high-pressure rocks from New Caledonia (Fig. 3) and other metamorphic terranes (Sakai et al. 1984; Sorenson 1991; Nagasaki and Enami 1998; Zack et al. 2002). We suggest that this zoning is the result of the episodic breakdown of minerals with varying trace-element contents. Hence, the trace element-rich allanite zones may have formed in response to lawsonite and titanite breakdown, and the zoisite zones may have grown during reactions involving trace-element-deficient minerals, such as chlorite, albite or amphibole. Metamorphic reactions may also be responsible for trace element zoning in garnet and other minerals. An example discussed above includes the MREE-rich rims on garnets in sample 1101 (Fig. 5) that are interpreted to have formed during conversion of titanite to rutile. It is clear that phases such as allanite, zircon and titanite play an important role in balancing trace element budgets during mineral breakdown reactions.

Implications for subduction-zone magmatism

There is a wealth of isotopic and geochemical evidence to show that arc magmas contain a significant proportion of slab-derived volatiles and trace elements (Perfit et al. 1980; Tera et al. 1986; Hawkesworth et al. 1993; Pearce and Peate 1995). Previous research demonstrated that the liberation of water is strongly linked to the breakdown of hydrous phases (Peacock 1993; Schmidt and Poli 1998). In contrast, it has been unclear whether or not trace element liberation is also related to the breakdown of trace element-rich phases. The most important finding of this study is the decoupling of trace element and fluid release at the transition from lawsonite blueschist to eclogite facies. At this transition, mafic rocks lose about 75% of the H_2O content still present at lawsonite blueschist conditions, whereas the investigated trace elements are redistributed among major and accessory phases. Without contributions from metamorphic breakdown reactions, the composition of slab fluids will primarily be determined by mineral/fluid partitioning systematics. The fluid-mobile LILE are hosted in phengite throughout the transition from lawsonite blueschist to eclogite facies conditions. Hence the mobility of these elements in fluids generated during breakdown of hydrous minerals is controlled by phengite/fluid partitioning. Although calculation of fluid compositions is beyond the scope of this paper, our data indicates that in the temperature range of 550–600 °C the 3% of fluid generated by dehydration of mafic rocks is not capable of removing large quantities of the investigated trace elements. Hence we suggest that significant trace element transport from the slab is only possible at higher temperatures and/or in zones with very high fluid/rock ratios. On this premise, we advocate an alternative model of fluxing of fluid and trace elements from the slab to the mantle wedge. During subduction, mafic rocks undergo conversion from blueschist to eclogite by dehydration of minerals such as lawsonite, amphibole and chlorite. Ultramafic rocks may also dehydrate by serpentinite breakdown (Ulmer and Trommsdorff 1995). The fluid released from these reactions may flow into relatively hot zones in the slab, such as the slab/mantle-wedge interface (Bebout and Barton 1989; Peacock 1993). Under these conditions, fluid may be capable of stripping trace elements from mafic rocks or may cause fluid-assisted partial melting of sedimentary rocks (Davies 1999). The latter case would produce a solute-rich (Si, Na, LILE) fluid or hydrous granitic melt (Hermann and Green 2001). These fluids or melts subsequently migrate into the mantle wedge and contribute to the generation and composition of arc magmas. In this scenario, the fluid component necessary for generation of arc magmas is sourced from dehydration of blueschist-facies mafic rocks and serpentinites, but the elements that are distinctively enriched in these magmas are largely derived from the sedimentary portion of the subducting slab. This model is consistent with the data presented here as well as the majority of geochemical, geophysical and petrological data concerning deep processes in subduction zones.

Conclusions

Based on the geochemical characteristics of a range of blueschist and eclogite samples from New Caledonia, we have determined some fundamental information concerning the distribution and behaviour of trace elements in subducting crust. This information is vital for understanding the transfer of elements from subducting slabs to the mantle wedge and hence, the composition of arc magmas. Under lawsonite blueschist-facies conditions, the distribution of trace elements in mafic and pelitic rocks of the slab is difficult to model due to the persistence of igneous and detrital minerals and the lack of equilibrium partitioning among metamorphic minerals. Nonetheless, important trace-element hosts include, lawsonite, allanite, titanite, phengite and zircon. At epidote blueschist to eclogite facies conditions, trace-element equilibrium may be attained and epidote (allanite or zoisite), phengite, garnet, rutile and zircon are the major trace-element hosts. The breakdown of hydrous minerals during conversion from blueschist to eclogite liberates significant amounts of water, but the investigated trace elements are completely redistributed into the newly formed minerals. We suggest that the flux of trace elements from the slab is not directly linked to mineral breakdown, but may be related to the production of hydrous fluids or melts formed during the infiltration of water into thermally elevated portions of the slab.

References

Abers GA (2000) Hydrated subducted crust at 100–250 km depth. Earth Planet Sci Lett 176:323–330

Aitchison J, Clarke GL, Meffre S, Cluzel D (1995) Eocene arc-continent collision in New Caledonia and implications for regional Southwest Pacific tectonic evolution. Geology 23:161–164

Arculus RJ, Lapierre H, Jaillard E (1999) Geochemical window into subduction and accretion processes: Raspas metamorphic complex, Ecuador. Geology 27:547–550

Bebout GE, Barton MD (1989) Fluid flow and measomatism in a subduction zone hydrothermal system: Catalina Schist terrane, California. Geology 17:976–980

Becker H, Jochum KP, Carlson RW (1999) Constraints from high-pressure veins in eclogites on the composition of hydrous fluids in subduction zones. Chem Geol 160:291–308

Becker H, Jochum KP, Carlson RW (2000) Trace element fractionation during dehydration of eclogites from high-pressure terranes and the implications for element fluxes in subduction zones. Chem Geol 163:65–99

Belousova EA, Walters S, Griffin WL, O'Reilly SY (2001). Trace-element signatures of apatites in granitoids from the Mt Isa Inlier, northwestern Queensland. Australian J Earth Sci vol. 48, pg 603–619

Black PM (1974) Oxygen isotope study of metamorphic rocks from the Ouegoa District, New Caledonia. Contrib Mineral Petrol 47:197–206

Black PM (1977) Regional high-pressure metamorphism in New Caledonia; phase equilibria in the Ouegoa District. Tectonophysics 43:89–107

Brenan JM, Shaw HF, Ryerson FJ, Phinney DL (1995) Mineral-aqueous fluid partitioning of trace elements at 900 degrees C and 2.0 GPa; constraints on the trace element chemistry of mantle and deep crustal fluids. Geochim Cosmochim Acta 59:3331–3350

Briggs RM, Kobe HW, Black PM (1977) High-pressure metamorphism of stratiform sulphide deposits from the Diahot region, New Caledonia. Miner Deposita 12:263–279

Brothers RN, (1985) Regional mid-Tertiary blueschist-eclogite metamorphism in northern New Caledonia. Geol Fr 1985:37–44

Carson CJ, Powell R, Clarke GL, (1999) Calculated mineral equilibria for eclogites in CaO-Na$_2$O-FeO-MgO-Al$_2$O$_3$-SiO$_2$-H$_2$O; application to the Pouebo Terrane, Pam Peninsula, New Caledonia. J Metamorph Geol 17:9–24

Carswell DA, Wilson RN, Zhai M (1996) Ultra-high pressure aluminous titanites in carbonate-bearing eclogites at Shuanghe in Dabieshan, central China. Mineral Mag 60:461–471

Clarke GL, Aitchison JC, Cluzel D (1997) Eclogites and blueschists of the Pam Peninsula, NE New Caledonia; a reappraisal. J Petrol 38: 843–876

Connolly JAD, Kerrick DM (2002) Metamorphic controls on seismic velocity of subducted oceanic crust at 100–250 km depth. Earth Planet Sci Lett 204:61–74

Davies JH (1999) The role of hydraulic fractures and intermediate-depth earthquakes in generating subduction-zone magmatism. Nature 398:142–145

Domanik KJ, Hervig RL, Peacock SM (1993) Beryllium and Boron in subduction zone minerals - an ion microprobe study. Geochim Cosmochim Acta 57:4997–5010

Domanik KJ, Holloway JR (1996) The stability and composition of phengitic muscovite and associated phases from 5.5 to 11 GPa; implications for deeply subducted sediments. Geochim Cosmochim Acta 60:4133–4150

Ellis DJ, Green DH (1979) An experimental study of the effect of Ca upon garnet-clinopyroxene Fe-Mg exchange equilibria. Contrib Mineral Petrol 71:13–22

Evans BW (1990) Phase relations of epidote-blueschists. Lithos 25:3–23

Fitzherbert JA, Clarke GL, Marmo BA, Powell R (2001) Metabasites from the Pam Peninsula, NE New Caledonia: development of regional blueschist to eclogite facies zonation. 6th Int Eclog Conf, 39 pp

Frost BR, Chamberlain KR, Schumacher JC (2001) Sphene (titanite); phase relations and role as a geochronometer. Chem Geol 172:131–148

Getty SR, Selverstone J (1994) Stable isotopic and trace element evidence for restricted fluid migration in 2 GPa eclogites. J Metamorph Geol 12:747–760

Graham CM, Powell R (1984) A garnet-hornblende geothermometer; calibration, testing, and application to the Pelona Schist, Southern California. J Metamorph Geol 2:13–31

Green TH, Hellman PL (1982) Fe-Mg partitioning between coexisting garnet and phengite at high pressure, and comments on a garnet-phengite geothermometer. Lithos 15:253–266

Hawkesworth CJ, Gallagher K, Hergt JM, and McDermott F (1993) Mantle and slab contributions in arc magmas. Annu Rev Earth Planet Sci 21:175–204

Hermann J (2002) Allanite: thorium and light rare earth element carrier in subducted crust. Chem Geol 192:289–306

Hermann J, Green DH (2001) Experimental constraints on high pressure melting in subducted crust. Earth Planet Sci Lett 188:149–168

Itaya T, Brothers RN, Black PM (1985) Sulfides, oxides and sphene in high-pressure schists from New Caledonia. Contrib Mineral Petrol 91:151–162

Kincaid C, Sacks IS (1997) Thermal and dynamical evolution of the upper mantle in subduction zones. J Geophys Res 102:12,295–12,315

Kirby SH, Engdahl ER, Denlinger RP (1996) Intermediate-depth intraslab earthquakes and arc volcanism as physical expressions of crustal and uppermost mantle metamorphism in subducting slabs. In: Bebout BE, Scholl DW, Kirby SH, Platt JP (eds) Subduction: top to bottom. American Geophysical Union, Washington, DC, pp. 195–214

Kogiso T, Tatsumi Y, Nakano S (1997) Trace element transport during dehydration processes in the subducted oceanic crust; 1, Experiments and implications for the origin of ocean island basalts. Earth Planet Sci Lett 148:193–205

Lin CH, Huang BS, Rau RJ (1999) Seismological evidence for a low-velocity layer within the subducted slab of southern Taiwan. Earth Planet Sci Lett 174:231–240

Liu J, Bohlen SR, Ernst WG (1996) Stability of hydrous phases in subducting oceanic crust. Earth Planet Sci Lett 143:161–171

Maurizot P, Eberle J-M, Habault C, Tessarolo C (1989) Notice explicative Sur La Feuille Pam-Ouegoa. BurRech Geol Mini Noumea

Messiga B, Tribuzio R, Bottazzi P, Ottolini L (1995) An ion microprobe study on trace element composition of clinopyroxenes from blueschist and eclogitized Fe-Ti-gabbros, Ligurian Alps, northwestern Italy; some petrologic considerations. Geochim Cosmochim Acta 59:59–75

Nagasaki A, Enami M (1998) Sr-bearing zoisite and epidote in ultra-high pressure (UHP) metamorphic rocks from the Su-Lu province, eastern China; an important Sr reservoir under UHP conditions. Am Mineral 83:240–247

Nishiyama T (1989) Kinetics of hydrofracturing and metamorphic veining. Geology 17:1068–1071

Okamoto K, Maruyama S (1999) The high-pressure synthesis of lawsonite in the MORB + H$_2$O system. Am Mineral 84 362–373

Ono S (1998) Stability limits of hydrous minerals in sediment and mid-ocean ridge basalt compositions; implications for water transport in subduction zones. J Geophys Res 103:18253–18267

Pawley AR, Holloway JR (1993) Water sources for subduction zone volcanism; new experimental constraints. Science 260:664–667

Peacock SM (1993) The importance of blueschist → eclogite dehydration reactions in subducting oceanic crust. Geol Soc Am Bull 105:684–694

Peacock SM (1996) Thermal and petrologic structure of subduction zones. In: Bebout BE, Scholl DW, Kirby SH, Platt JP (eds) Subduction: top to bottom. American Geophysical Union, Washington, DC, pp 119–133

Pearce JA, Peate DW (1995) Tectonic implications of the composition of volcanic arc magmas. Ann Rev Earth Planet Sci 23:251–285

Perfit MR, Gust DA, Bence AE, Arculus RJ, Taylor SR (1980) Chemical characteristics of island-arc basalts; implications for mantle sources. Chem Geol 30:227–256

Philippot P, Selverstone J (1991) Trace-element-rich brines in eclogitic veins: implications for fluid composition and transport during subduction. Contrib Mineral Petrol 106:417–430

Plank T, Langmuir CH (1998) The chemical composition of subducting sediment and its consequences for the crust and mantle. Chem Geol 145:325–394

Poli S, Schmidt MW (1995) H$_2$O transport and release in subduction zones - experimental constraints on basaltic and andesitic systems. J Geophys Res 100:22299–22314

Poli S, Schmidt MW (2002) Petrology of subducted slabs. Annu Rev Earth Planet Sci 30:207–235

Rawling TJ, Lister GS (1999) Oscillating modes of orogeny in the Southwest Pacific and the tectonic evolution of New Caledonia. In: Ring TU, Brandon MS, Lister G, Willett SD (eds) Exhumation processes; normal faulting, ductile flow and erosion. Geol Soc Lond Spec Publ 154:109–127

Rawling TJ, Lister GS (2002) Large-scale structure of the eclogite-blueschist belt of New Caledonia. J Struct Geol 24:1239–1258

Rollinson H (1993) Using geochemical data: evaluation, presentation, interpretation. Longman, London

Rubatto D (2002) Zircon trace element geochemistry; partitioning with garnet and the link between U-Pb ages and metamorphism. Chem Geol 184:123–138

Rubatto D, Hermann J (2003) Zircon formation during fluid circulation in eclogites (Monviso, Western Alps): implications for Zr and Hf budgets in subduction zones. Geochim Cosmochim Acta 67:2173–2187

Sakai C, Higashino T, Enami M (1984) REE-bearing epidote from Sanbagawa pelitic schists, central Shikoku, Japan. Geochem J 18:45–53

Sassi P, Harte B, Carswell DA, Yujing H (2000) Trace element distribution in central Dabie eclogites. Contrib Mineral Petrol 139:298–315

Scambelluri M, Philippot P (2001) Deep fluids in subduction zones. Lithos 55:213–227

Schmidt MW, Poli S (1998) Experimentally based water budgets for dehydrating slabs and consequences for arc magma generation. Earth Planet Sci Lett 163:361–379

Shatsky VS, Kozmenko OA, Sobolev NV (1990) Behaviour of rare-earth elements during high-pressure metamorphism. Lithos 25:219–226

Sorensen SS (1991) Petrogenetic significance of zoned allanite in garnet amphibolites from a paleosubduction zone—Catalina Schist, southern California. Am Mineral 76: 589–601

Sorensen SS, Grossman JN (1989) Enrichment of trace elements in garnet amphibolites from a paleo-subduction zone; Catalina Schist, Southern California. Geochim Cosmochim Acta 53: 3155–3177

Sorensen SS, Grossman JN, Perfit MR (1997) Phengite-hosted LILE enrichment in eclogite and related rocks; implications for fluid-mediated mass transfer in subduction zones and arc magma genesis. J Petrol 38: 3–34

Sun SS, McDonough WF (1989) Chemical and isotopic systematics of oceanic basalts; implications for mantle composition and processes. In: Saunders AD, Norry MJ (eds) Magmatism in the ocean basins. Geol Soc Lond Spec Publ 42:313–345

Tatsumi Y, Hamilton DL, Nesbitt RW (1986) Chemical characteristics of fluid phase released from a subducted lithosphere and origin of arc magmas; evidence from high-pressure experiments and natural rocks. J Volcanol Geotherm Res 29:293–309

Taylor SR, McLennan SM (1985) The continental crust: its composition and evolution. Blackwell, Oxford

Tera F, Brown L, Morris J, Sacks IS, Klein J, Middleton R (1986) Sediment incorporation in island-arc magmas; inferences from Be-10. Geochim Cosmochim Acta 50:535–550

Thöni M, Jagoutz E (1992) Some new aspects of dating eclogites in orogenic belts: Sm-Nd, Rb-Sr, and Pb-Pb isotopic results from the austoalpine Saualpe and Koralpe type-locality (Carinthia/Styria, southeastern Austria). Geochim Cosmochim Acta 56:347–368

Tribuzio R, Messiga B, Vannucci R, Bottazzi P (1996) Rare earth element redistribution during high-pressure-low-temperature metamorphism in ophiolitic Fe-gabbros (Liguria, northwestern Italy); implications for light REE mobility in subduction zones. Geology 24:711–714

Tribuzio R, Tiepolo M, Thirlwall MF (2000) Origin of titanian pargasite in gabbroic rocks from the Northern Apennine ophiolites (Italy): insights into the late-magmatic evolution of a MOR-type intrusive sequence. Earth Planet Sci Lett 176:281–293

Troitzsch U, Ellis DJ (2002) Thermodynamic properties and stability of AlF-bearing titanite $CaTiOSiO_4$–Ca-$AlFSiO_4$. Contrib Mineral Petrol 142:543–563

Ueno T (1999) REE-bearing sector-zoned lawsonite in the Sanbagawa pelitic schists of the eastern Kii Peninsula, central Japan. Euro J Mineral 11:993–998

Ulmer P, Trommsdorff V (1995) Serpentine stability to mantle depths and subduction-related magmatism. Science, 268:858–861

White WM (2001). Geochemistry. http://www.geo.cornell.edu/geology/classes/geo455/Chapters.HTML

Wilson M (1989) Igneous petrogenesis; a global tectonic approach. Unwin Hyman, London

Xiao Y, Hoefs J, van den Kerkhof AM, Fiebig J, Zheng Y (2000) Fluid history of UHP metamorphism in Dabie Shan, China: a fluid inclusion and oxygen isotope study on the coesite-bearing eclogite from Bixiling. Contrib Mineral Petrol 139:1–16

Yokoyama K, Brothers RN, Black PM (1986) Regional eclogite facies in the high-pressure metamorphic belt of New Caledonia. In: Evans BW, Brown EH (eds) Blueschists and eclogites. Geol Soc Am Mem 164:407–423

Zack T, Foley SF, Rivers T (2002) Equilibrium and disequilibrium trace element partitioning in hydrous eclogites (Trescolmen, Central Alps). J Petrol 43: 1947–1974